ALGODE TOKYO 2011

Proceedings of the International Symposium on Algorithmic Design for Architecture and Urban Design,
ALGODE TOKYO 2011
March 14-16, 2011, Tokyo, Japan

Multiobjective shape optimization of latticed shells for elastic stiffness and uniform member lengths

Makoto OHSAKI[1*], Shinnosuke FUJITA[2]

[1*]Deptartment of Architecture, Hiroshima University
1-4-1, Kagamiyama, Higashi-Hiroshima 739-8527, Japan
ohsaki@hiroshima-u.ac.jp

[2] Kanebako Structural Engineers, Japan

Abstract

A multiobjective optimization approach is presented for shape design of latticed shells. The objective functions are the strain energy under static loads and the variance of member lengths. Numerical results are shown for the latticed shells with three types; namely, triangular grid, quadrilateral grid, and hexagonal grid. The topology of each grid is fixed, and the locations of control points or the nodal coordinates are considered as design variables. The constraint approach is used for multiobjective optimization. Optimization results show that the triangular-grid shell with uniform member lengths turn out to be a cylindrical surface with equilateral triangles. The optimal shapes for quadrilateral grids are highly dependent on the initial solutions, and there exists a kind of bifurcation for the set of local optimal solutions in the objective function space. Finally, various shapes with uniform member lengths are found for the latticed shells with hexagonal grids.

Keywords: Shape optimization, latticed shell, strain energy, geometrical property

1 Introduction

There exist many papers on shape optimization of free-form shells modeled by parametric surfaces such as Bézier surfaces and NURBS (Non-Uniform Rational B-Spline) surfaces [1]. However, most of them are concerned with mechanical properties. In architectural design, we have to consider non-mechanical properties including aesthetic properties and constructability that are difficult to define in explicit forms. Especially for a free-form shell, it is very important to formulate the design problem considering mechanical and non-mechanical performances, because there exists a strong interaction between its shape and mechanical performance [2-4].

Shape optimization has also been studied for latticed shells defined by parametric surfaces [5,6]. For a latticed shell, locations of nodes and members are also to be optimized [7], and the constructability plays a key role as the non-mechanical performance. Ogawa *et al*. [8] maximized the linear buckling load under constraint on the variances of lengths of members that are classified into several groups. However, in their work, the surface shape is fixed; therefore, the latticed shell with uniform member lengths was not obtained.

It is very important in practical design and construction of latticed shell that the number of different parts including joints and members should be restricted to reduce the cost and period for construction. It is well known that the grids with uniform mesh can be generated for regular surfaces such as sphere and cylinder [9]. Recently, the latticed shells with hexagonal grids have been extensively studied [10,11]. Efficient covering of free-form shells with regular-shaped panels has also been studied in view of smoothness and cost [12,13].

In this study, an approach is presented for multiobjective shape optimization of latticed shells defined using parametric or non-parametric surface. The objective functions are the strain energy under self-weight and the variance of member lengths. Numerical results are shown for the latticed shells with three types; namely, triangular grid, quadrilateral grid, and hexagonal grid. The topology of each grid is fixed, and the locations of control points or the nodal coordinates are considered as design variables. The constraint approach is used for multiobjective optimization. If a feasible solution with uniform member lengths exists, then the strain energy is minimized under constraint on the member lengths; otherwise, the variance of member length is minimize under constraint on strain energy. Optimization results show that the triangular grid with uniform member lengths turns out to be a cylindrical surface with equilateral triangles. It is also shown that the optimal shapes for quadrilateral grid are highly dependent on the initial solutions, and there exists a kind of bifurcation for the local optimal solutions in the objective function space. Finally, various shapes with uniform member lengths are found for the latticed shells with hexagonal grids.

2 Formulation of optimization problem

We minimize the strain energy under static loads to improve stiffness of the latticed shell. The variance of member lengths is also minimized to improve constractability. Therefore, we have two objective functions that are to be minimized; i.e., the optimization problem is formulated as a multiobjective problem.

In the following examples of latticed shells with triangular and quadrilateral grids, the surface is described by Bézier surfaces, and the nodal locations are defined by specifying the coordinates in the parameter plane. The surface of the hexagonal-grid shell, by contrast, is defined by the coordinates of each node. In either case, the vector of variable components of coordinates of control points or nodes is denoted by $\mathbf{x}$. Let $l_k(\mathbf{x})$ denote the length of member k, which is a function of the design variable vector $\mathbf{x}$. The number of members and the average of member lengths are denoted by m and $l_{\text{ave}}(\mathbf{x})$, respectively. The deviation $g(\mathbf{x})$ of member lengths is defined as

$$g(\mathbf{x}) = \sum_{k=1}^{m} (l_k(\mathbf{x}) - l_{\text{ave}}(\mathbf{x}))^2 \tag{1}$$

A latticed shell with uniform member lengths is obtained by assigning the constraint $g(\mathbf{x}) = 0$.

Let $\mathbf{K}(\mathbf{x})$ and $\mathbf{d}(\mathbf{x})$ denote the stiffness matrix and the nodal displacement vector under the specified static loads. The strain energy $f(\mathbf{x})$ is defined as

$$f(\mathbf{x}) = \frac{1}{2}\mathbf{d}(\mathbf{x})^{\mathrm{T}}\mathbf{K}(\mathbf{x})\mathbf{d}(\mathbf{x}) \tag{2}$$

which is a half of the compliance that is usually used as the objective function of a structural optimization problem. We can obtain a stiff structure by minimizing $f(\mathbf{x})$.

Let $L(\mathbf{x})$ denote the sum of member lengths. The following constraint is given in order to prevent the optimization algorithm to converge to an optimal shape with very small rise:

$$L(\mathbf{x}) = L_0 \tag{3}$$

where L_0 is the value of $L(\mathbf{x})$ of the initial shape for optimization. Note that Eq. (3) is equivalent to the constraint on the total structural volume, if all members have the same cross-section.

Hence, the multiobjective optimization problem to obtain a stiff latticed shell with uniform member lengths is formulated as

Problem MOP: Minimize $f(\mathbf{x})$ and $g(\mathbf{x})$
subject to $L(\mathbf{x}) = L_0$

There have been various approaches to multiobjective optimization problem, among which the linear-weighted-sum approach and constraint approach are often used. Suppose minimizing $g(\mathbf{x})$ is more important than minimizing $f(\mathbf{x})$. In this case, $f(\mathbf{x})$ is minimized with a small bound for $g(\mathbf{x})$. Since the best value for $g(\mathbf{x})$ is 0, we first solve the following single-objective optimization problem:

Problem MF: Minimize $f(\mathbf{x})$
subject to $g(\mathbf{x}) = 0$
$L(\mathbf{x}) = L_0$

However, this problem may have no feasible solution depending on the specified topology, initial shape, and definition of the variables. Therefore, in such case, the objective and constraint functions are exchanged as follows:

Problem MG: Minimize $g(\mathbf{x})$
subject to $f(\mathbf{x}) = \overline{f}$
$L(\mathbf{x}) = L_0$

where $\overline{f}$ is the specified value of strain energy. Since we have no clue for an appropriate value of $\overline{f}$, we solve Problem MG for various values of $\overline{f}$ in accordance with the standard procedure of the constraint approach.

It may be possible to minimize the difference between the maximum and minimum member lengths to obtain a latticed shell with uniform lengths. However, in this case, we have the following $2m$ inequality constraints:

$$l_{\min} \leq l_k \leq l_{\max}\,, \qquad (k = 1, \ldots, m) \tag{4}$$

where $l_{\max}$ and $l_{\min}$ are the maximum and minimum values of member lengths, which are considered as auxiliary variables. Therefore, the number of constraints, and, consequently, the computational cost is very large compared with those of Problems MF and MG. Hence, we use the formulation MF or MG.

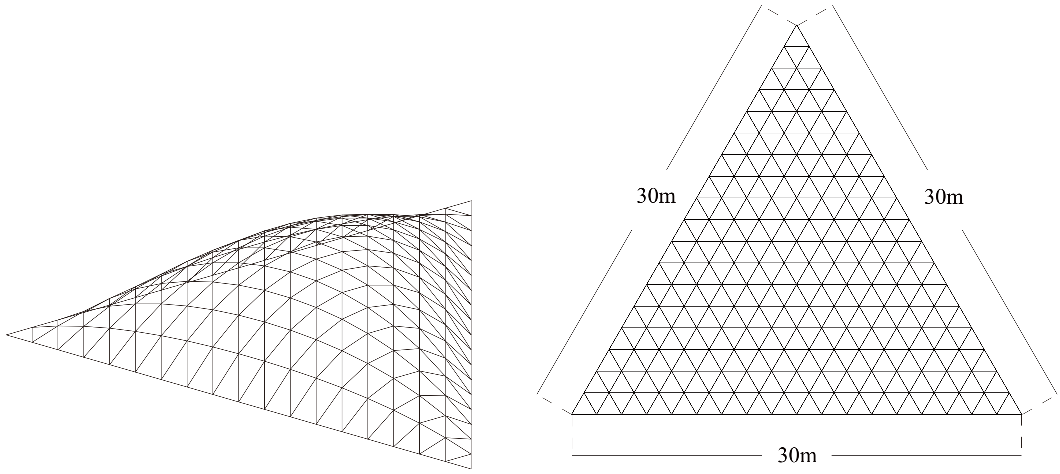

(a) *(b)*
Fig. 1: A latticed shell with triangular grids; (a) diagonal view, (b) plan.

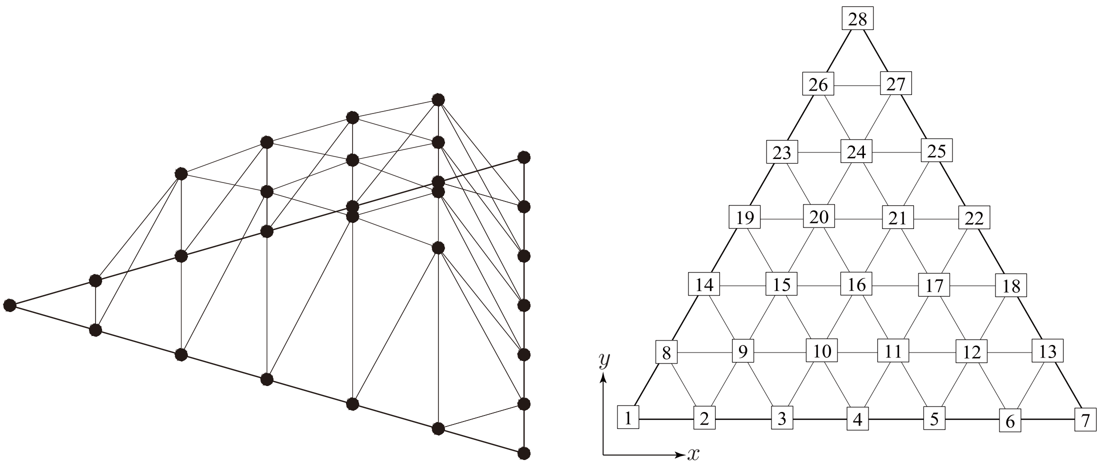

(a) *(b)*
Fig. 2: Control polygon of the latticed shell with triangular grids;
(a) diagonal view, (b) plan with numbers of control points.

ALGODE TOKYO 2011

Proceedings of the International Symposium on Algorithmic Design for Architecture and Urban Design,
ALGODE TOKYO 2011
March 14-16, 2011, Tokyo, Japan

3 Latticed shells with various grid shapes

In this section, latticed shells with triangular, quadrilateral, and hexagonal grids are defined in the space with (x, y)-coordinates on the horizontal plane, and z-coordinate in the upper vertical direction. The nodal locations of triangular- and quadrilateral-grid shells are defined by specifying the coordinates in the parameter plane.

3.1 Triangular grid

Consider a latticed shell with triangular grids as shown in Fig. 1 with a plan of 30 m equilateral triangle. The lines in Fig. 1 represent the members that are rigidly connected at the joints. The surface is defined by the 6-order Bézier triangle. The control polygon is shown in Fig. 2. The nodal displacements under static loads are fixed at the three corners.

The design variables are the (x, y, z)-coordinates of the control points satisfying the following requirements:

(a) Fix the points at the three corners.
(b) Fix the point 28, and move the points 1, ..., 7 in x-direction only along the boundary.

In the numerical examples, these cases are designated as Case-a and Case-b.

3.2 Quadrilateral grid

Consider a latticed shell with quadrilateral grid as shown in Fig. 3 with 30 m × 30 m square plan. The surface is defined by the 6×6 tensor product Bézier surface. The control polygon is shown in Fig. 4. The following two boundary conditions are considered for displacements under static loads:

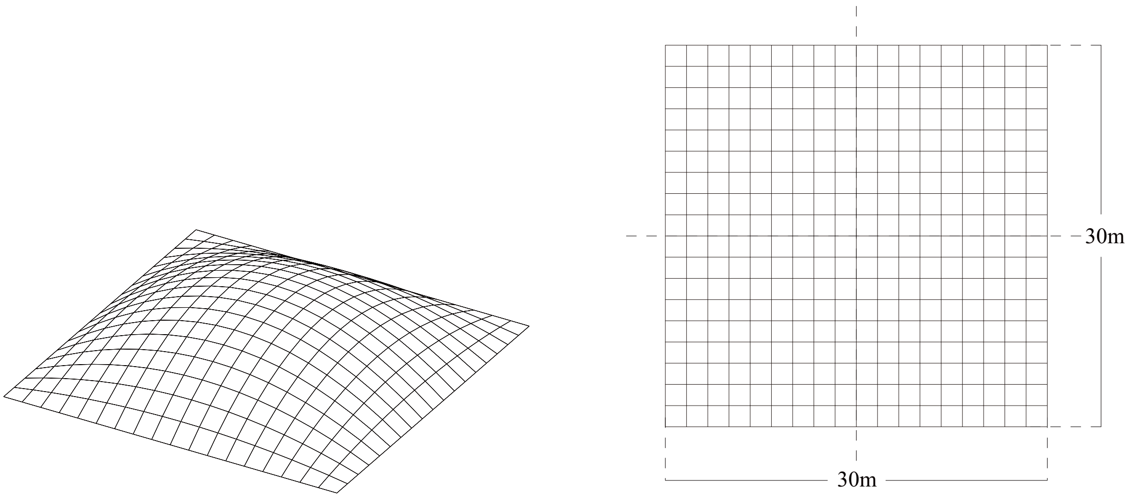

(a) *(b)*

Fig. 3: A latticed shell with quadrilateral grids; (a) diagonal view, (b) plan.

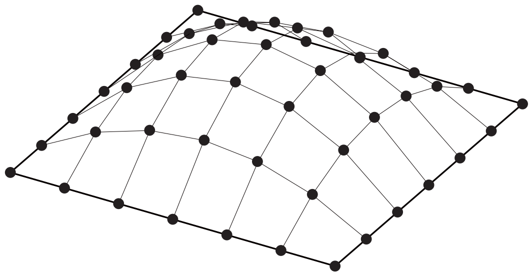

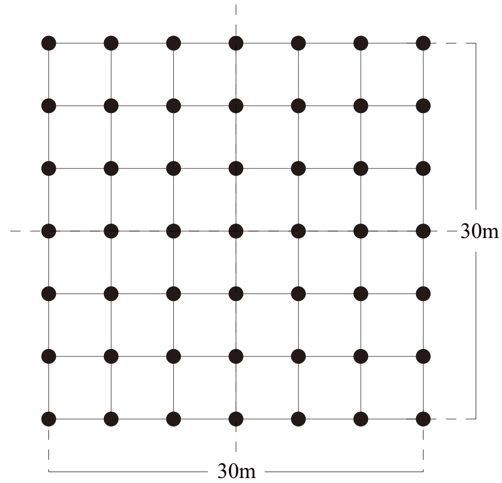

(a) *(b)*

Fig. 4: Control polygon of the latticed shell with quadrilateral grids; (a) diagonal view, (b) plan.

1. Fixed supports at the four corners.
2. Pin supports along the boundary.

The design variables are the (x, y, z)-coordinates of the control points satisfying the following requirements:

(a) Fix the points at the four corners.
(b) Fix the points at the four corners, and move the remaining points on the boundary in z-direction and along the boundary.
(c) Fix the points at the four corners, and move the remaining points on the boundary in xy-plane.

In the numerical examples, these cases are designated as Case-1-a, Case-2-b, etc.

3.3 Hexagonal grid

Consider a latticed shell with hexagonal grid as shown in Fig. 5 with 30 m between the supports. We do not use a Bézier surface for this type; i.e., the nodal coordinates are directly optimized. The node numbers are shown in Fig. 6 on the xy-plane. The following two boundary conditions are considered for nodal displacements:

1. Fixed supports at the six corners.
2. Pin supports along the boundary.

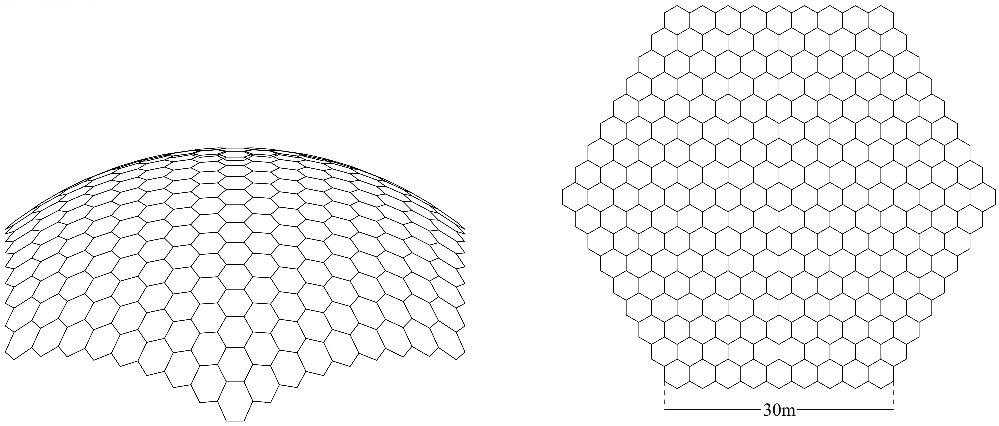

(a) *(b)*

Fig. 5 A latticed shell with hexagonal grids; (a) diagonal view, (b) plan.

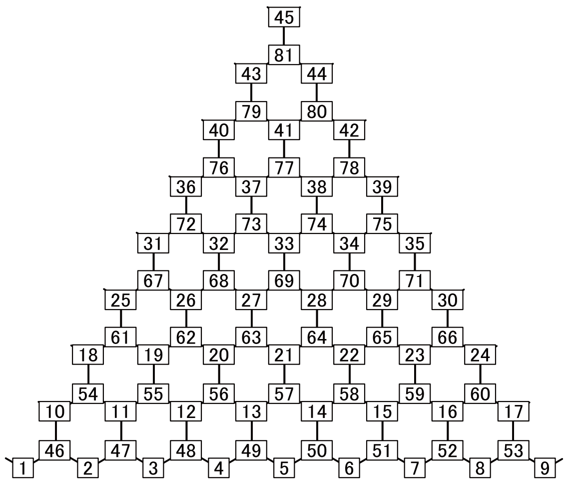

Fig. 6: Node numbers of a latticed shell with hexagonal grids.

The design variables are the (x, y, z)-coordinates of the nodes satisfying the following requirements:

(a) Nodes 1 and 9 can move only in x-direction.
(b) Nodes 1 and 9 can move only in x-direction, and nodes 2, ..., 8 can move only in xy-plane.
(c) Nodes 1 and 9 can move only in x-direction, and z-coordinates of nodes 1, ..., 9 are fixed at 0.

In the numerical examples, these cases are designated as Case-1-a, Case-2-b, etc.

4 Optimization results

The members consist of tubes with external radius 135.2 mm and thickness 4 mm, which are rigidly connected at the joints. The elastic modulus is 210 kN/mm^2, and Poisson's ratio is 0.3. The structure is subjected to self-weight with weight density 77 kN/m^3. Each member is modeled as a standard beam-column element with cubic interpolation function.

The library SNOPT Ver. 7.2 [13], which utilizes sequential quadratic programming, is used for optimization, where the sensitivity coefficients of the static displacements and the member lengths with respect to the nodal coordinates are computed analytically. The sensitivity coefficients of nodal coordinates with respect to the coordinates of control points can be computed easily in the same manner as described in Ref. [3].

4.1 Triangular grid

Optimal shapes are found for two cases with different variable requirements. The optimization results are summarized in Table 1, where $N^{\mathrm{t}}_{\max}$ is the maximum tensile axial force, $N^{\mathrm{c}}_{\max}$ is the maximum absolute value of compressive axial force, $M_{\max}$ is the maximum absolute value of bending moment, and $d_{\max}$ is the maximum nodal deflection. All the solutions are found from the initial shape in Fig. 1, which is designated as 'Initial' in Table 1.

For Case-a with strict variable requirement, there is no feasible solution for Problem MF. Therefore, Problem MG is solved with $\overline{f} = 1.0$ to find the optimal shape as shown in Fig. 7(a). The value of $l_{\max} - l_{\min}$ is 9.544 mm, which is far less than the initial value 1054.0 mm, but is not sufficiently small.

If we increase the number of variables and solve Case-b, the optimal shape of Problem MF is as shown in Fig. 7(b) with uniform member lengths. Note that the small value 4.667×10^{-1} mm of $l_{\max} - l_{\min}$ in Table 1 means that the member lengths are almost uniform with a small tolerance allowed by SNOPT. We can see from Fig. 7(b) that the optimal solution with uniform member lengths have cylindrical shape, and each grid turns out to be an equilateral triangle. Therefore, the requirement of uniform member lengths is too strict for a latticed shell with triangular grids to generate solutions with various shapes.

Table 1: Properties of optimal solutions of triangular grids.

	Initial	Case-a	Case-b
f (kN·m)	1.308	1.0	5.200×10^{-1}
g (m^2)	–––	1.940×10^{-3}	0.0
$l_{\max} - l_{\min}$ (mm)	1054.0	9.544	4.667×10^{-1}
$N^{\mathrm{t}}_{\max}$ (kN)	76.21	19.66	30.25
$N^{\mathrm{c}}_{\max}$ (kN)	84.83	43.10	74.13
$M_{\max}$ (k·Nm)	24.72	12.45	6.212
$d_{\max}$ (mm)	20.42	32.73	34.31

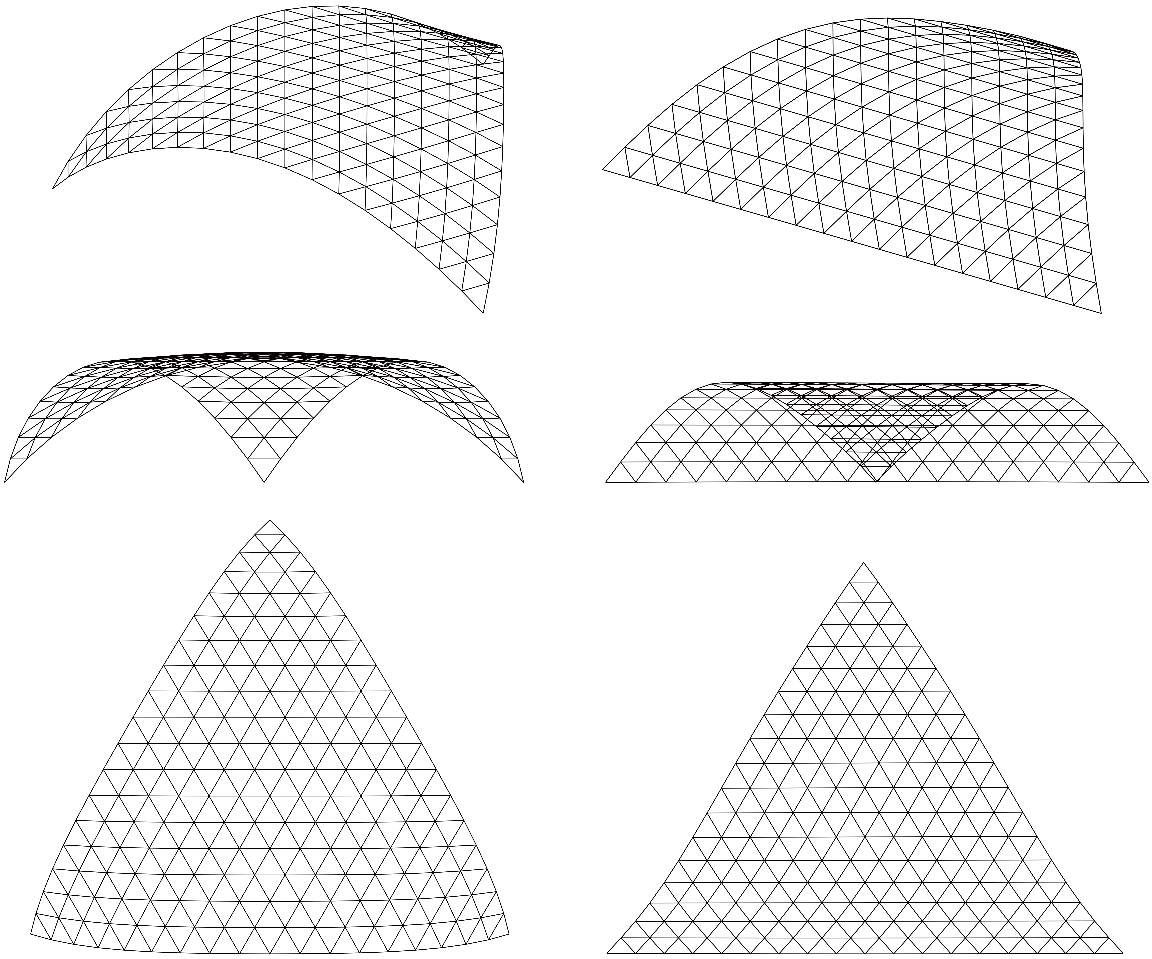

(a) *(b)*

Fig. 7: Optimal shapes of triangular grids; (a) Case-a (MG), (b) Case-b (MF).

Table 2: Properties of optimal solutions of quadrilateral grids.

	Case-1-0	Case-1-a	Case-1-b	Case-2-0	Case-2-a	Case-2-c
f (kN·m)	8.226	4.162×10^{-1}	1.270	3.225×10^{-2}	8.443×10^{-3}	0.06
g (m^2)	–––	0.0	0.0	0.0	0.0	4.155×10^{-2}
$l_{\max}-l_{\min}$ (mm)	422.2	9.248×10^{-1}	7.277×10^{-2}	422.2	4.258×10^{-1}	3.427
$N^{\mathrm{t}}_{\max}$ (kN)	17.66	0.0	0.0	0.0	0.0	12.14
$N^{\mathrm{c}}_{\max}$ (kN)	56.65	55.13	51.63	6.909	3.717	10.64
$M_{\max}$ (k·Nm)	36.74	4.641	7.878	5.579×10^{-1}	1.557×10^{-1}	8.169×10^{-1}
$d_{\max}$ (mm)	104.7	6.674	28.30	8.401×10^{-1}	3.353×10^{-1}	2.996

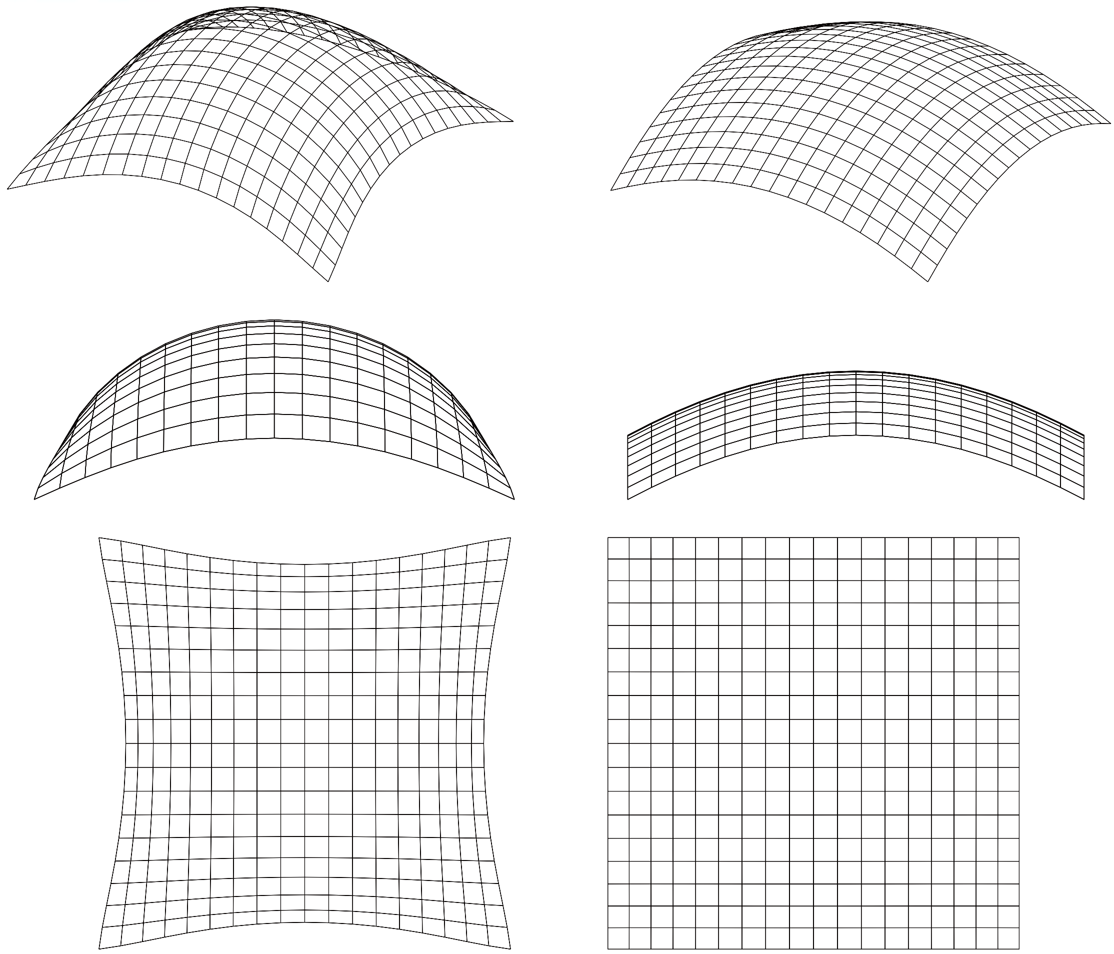

(a) *(b)*

Fig. 8: Optimal shapes for Case 1 of quadrilateral grids; (a) Case-1-a (MF), (b) Case-1-b (MF).

4.2 Quadrilateral grid

Optimal shapes are found for six cases with two boundary conditions and three variable requirements. The optimization results are summarized in Table 1, where Case-1-0 and Case-2-0 are the initial solutions for the two cases. All the solutions are found from the initial shape in Fig. 3.

The optimal shape of Problem MF for Case-1-a is shown in Fig. 8(a). As seen in Table 1, the optimal shape has uniform lengths and much larger stiffness (smaller strain energy) than the initial shape. The maximum bending moment is drastically reduced, and the vertical loads are resisted mainly through the compressive forces of members. The nodes move to the center as the result of optimization, which leads to in a smaller interior space. Therefore, we fix the boundary and obtain the optimal shape for Case-1-b as shown in Fig. 8(b), which has a round shape. Hence, the interior space is retained, although it has a little smaller stiffness (larger strain energy) than Case-1-a as listed in Table 1. Note that the members intersect perpendicularly in the plan view; hence, the number of different types of connections can be reduced by optimization. By contrast, for Case-2-a with different displacement boundary conditions, the optimal shape is as shown in Fig. 9(a), which is a little different from Case-1-a, but it also has a smaller interior space than the initial shape.

So far, we solved Problem MF, because there exists a feasible solution that has uniform member lengths. However, for Case-2-c, where the control points on the boundary can move only on the xy-plane, we could not find a solution with uniform member lengths. Therefore, we next solve Problem MG with $\overline{f} = 0.06$ to find the optimal shape as shown in Fig. 9(b). The difference between the maximum and minimum member lengths is 3.4 mm, which is small enough to regard that the member lengths are almost uniform. However, surface is not symmetric with respect to xz - and yz-planes, but has a rotational symmetry in 180 degrees around the center. This fact indicates that designing a latticed shell with uniform member lengths and an appropriate symmetry conditions is a very difficult requirement for the quadrilateral grids.

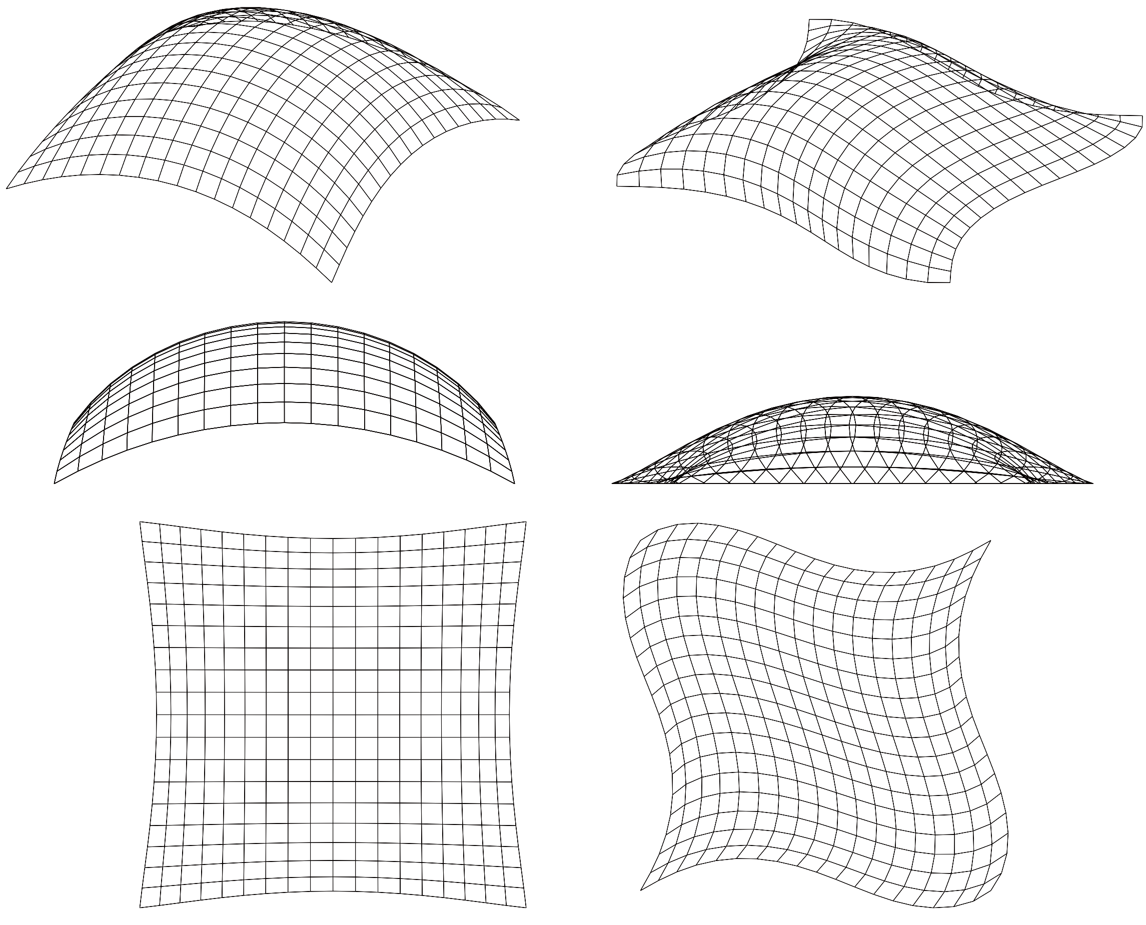

(a) *(b)*

Fig. 9: Optimal shapes for Case 2 of quadrilateral grids;
(a) Case-2-a (MF), (b) Case-2-c (MG).

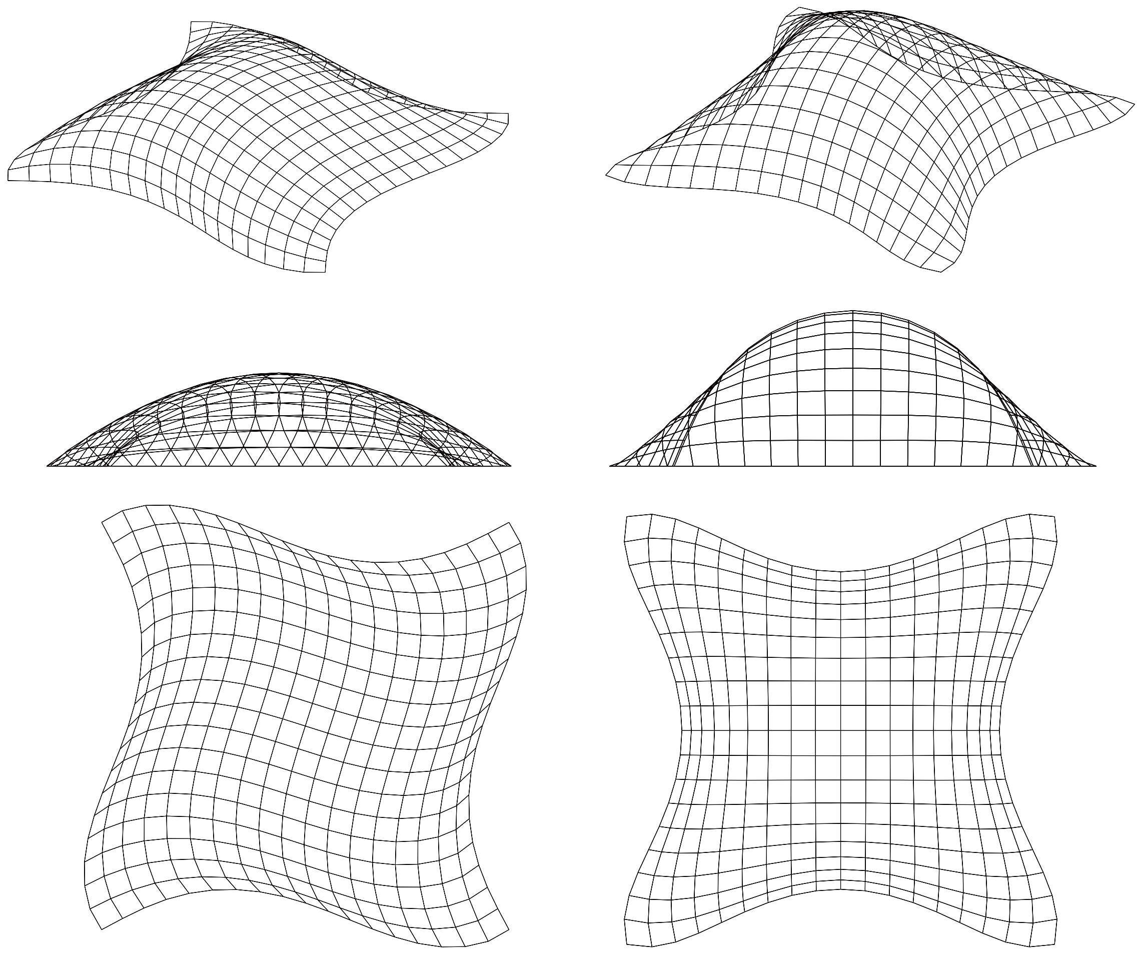

(a) *(b)*

Fig. 10: Optimal shapes for Case-2-c of quadrilateral grids;
(a) $\bar{f} = 0.04$, *(b)* $\bar{f} = 0.005$.

In order to investigate the uniqueness and symmetry of optimal shapes, we next solve Problem MG with different upper bounds of strain energy. The optimal shape for Case-2-c with $\bar{f} = 0.04$ and 0.005 (kN·m) are shown in Fig. 10(a) and (b), respectively. As is seen, the optimal shape strongly depends on the value of $\bar{f}$. The objective values for $\bar{f} = 0.04$ and 0.005 are 1.531×10^{-3} and 2.248×10^{-1} (m^2), respectively. Therefore, a strict requirement for stiffness leads to a non-uniformness of the member lengths and reduction of symmetry.

The objective values of Problem MG with different values of $\bar{f}$ and initial solutions are listed in Fig. 11, which shows a strong dependence of optimal solution on the initial solution. The two curves in Fig. 11 correspond to the two types in Fig. 10(a) and (b). Therefore, there exists a kind of bifurcation of the local optimal solutions in the objective function space.

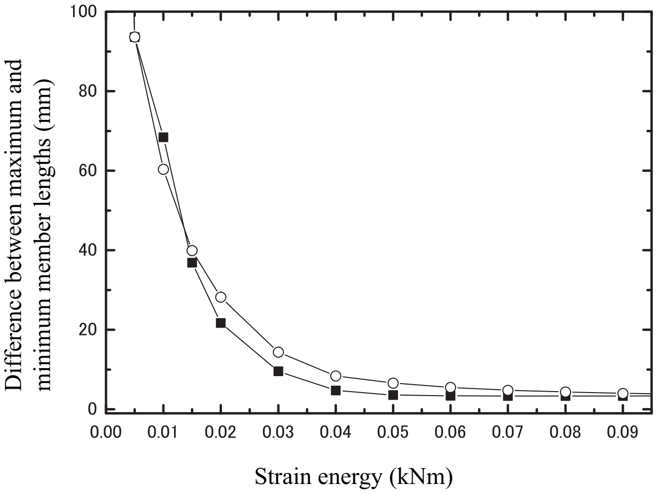

Fig. 11: Strain energy and the difference between maximum and minimum member lengths of optimal shapes obtained from optimal shapes for different values of $\overline{f}$; ■: $\overline{f} = 0.06$, □: $\overline{f} = 0.04$.

Table 3: Properties of optimal solutions of hexagonal grids.

	Case-1-0	Case-1-a	Case-1-b	Case-2-0	Case-2-a	Case-2-c
f (kN·m)	2.750	8.689×10^{-2}	8.804×10^{-2}	7.765×10^{-2}	2.745×10^{-2}	5.488×10^{-2}
g (m^2)	–––	0.0	0.0	0.0	0.0	0.0
$l_{\max} - l_{\min}$ (mm)	536.2	2.850×10^{-3}	4.158×10^{-3}	536.2	3.265×10^{-3}	5.229×10^{-3}
$N^{\mathrm{t}}_{\max}$ (kN)	6.562×10^{-1}	0.0	0.0	0.0	0.0	0.0
$N^{\mathrm{c}}_{\max}$ (kN)	30.28	25.76	26.99	6.898	7.295	7.501
$M_{\max}$ (k·Nm)	12.75	1.791×10^{-1}	6.228	6.412×10^{-1}	1.016×10^{-1}	8.872×10^{-2}
$d_{\max}$ (mm)	34.64	1.350	15.85	6.214	6.136×10^{-1}	1.114

4.3 Hexagonal grid

The optimization results for the hexagonal grids are summarized in Table 1. All the solutions are found from the initial shape in Fig. 5.

The optimal solution of Problem MF for Case-1-a is as shown in Fig. 12(a), which has uniform member lengths and large stiffness as listed in Table 1. As seen in Fig. 12(a), the nodes move to the center, which results in a smaller interior space. Therefore, we fix the boundary and obtain the optimal shape for Case-1-b as shown in Fig. 12(b), which has a smooth shape.

The optimal shape shown in Fig. 13(a) for Case-2-c also has uniform member lengths. The boundary nodes moved inside on the xy-plane, which results in irregular shape and small interior space. The optimal solution for Case-2-d also has uniform member lengths as shown in Fig. 13(b). Therefore, a latticed shell with hexagonal grids has a good ability for adjusting member length while retaining the stiffness. Furthermore, the optimal shapes have no tensile axial force and much smaller bending moments.

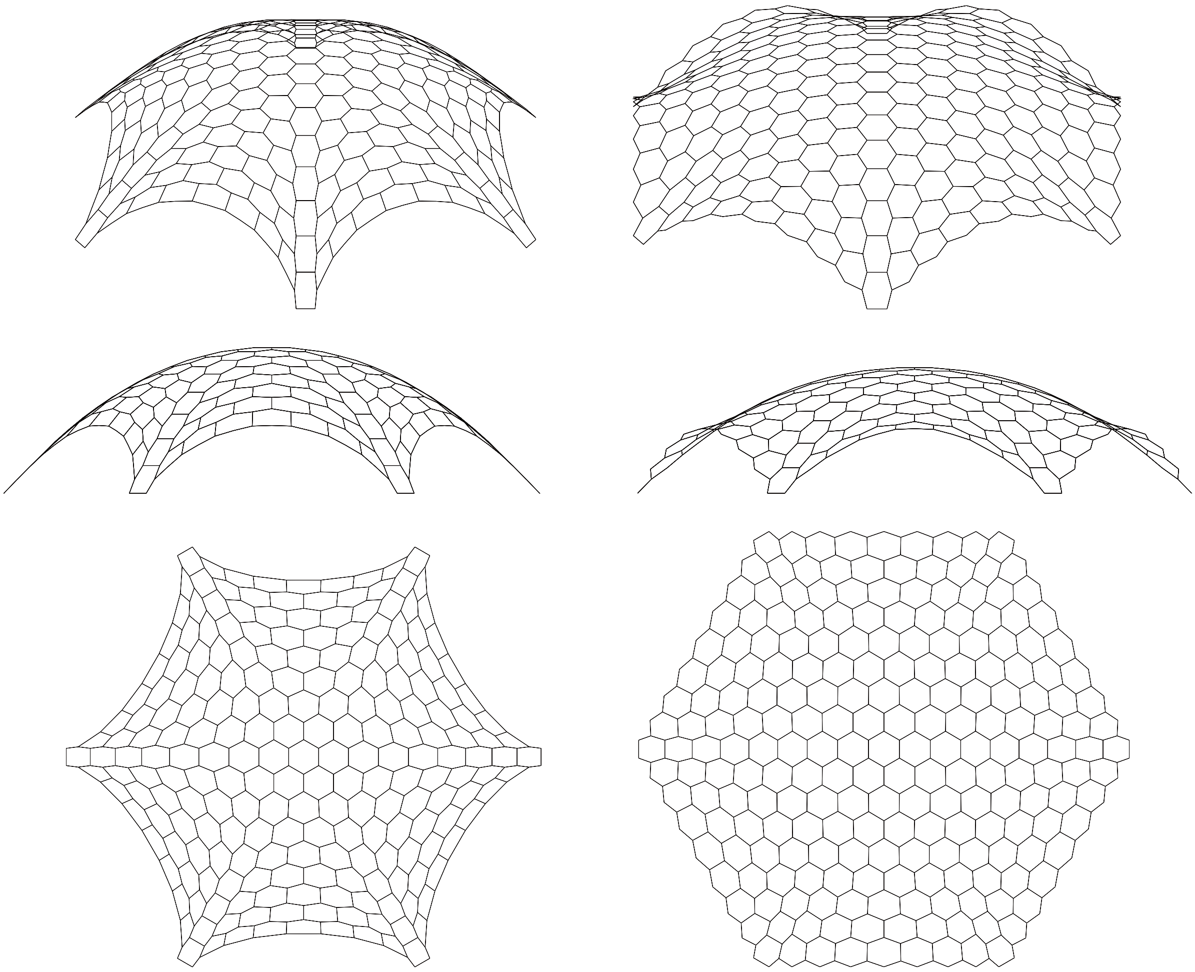

(a) *(b)*

Fig. 12: Optimal shapes for Case 1 of hexagonal grids; (a) Case-1-a (MF), (b) Case-1-b (MF).

5 Conclusions

An approach has been presented for multiobjective shape optimization of latticed shells. The objective functions are the strain energy under self-weight and the variance of member lengths.

Optimal shapes has been found for the latticed shells with triangular, quadrilateral, and hexagonal grids. Bézier surfaces are used for triangular and quadrilateral grids. The topology of each grid is fixed, and the locations of control points or the nodal coordinates are considered as design variables.

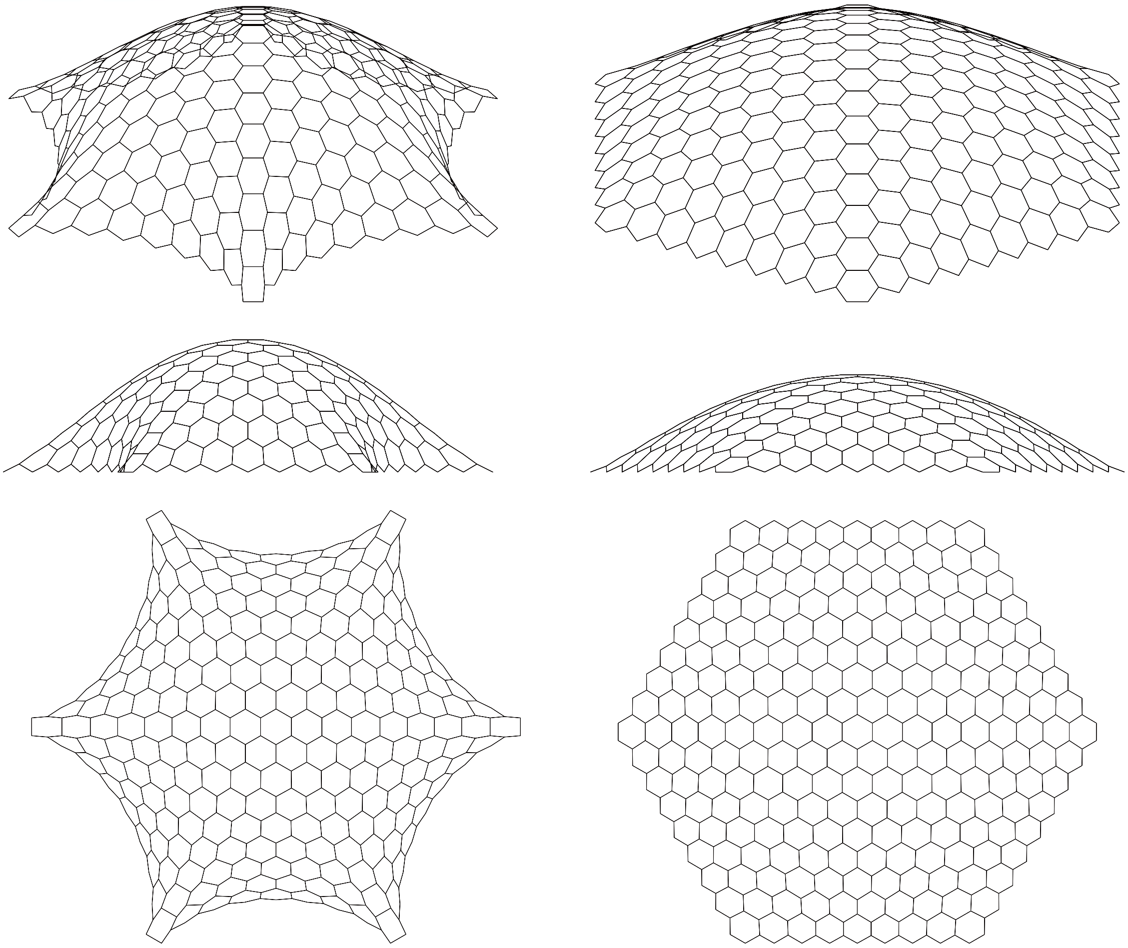

(a) *(b)*

Fig. 13: Optimal shapes for Case 2 of hexagonal grids; (a) Case-2-c (MF), (b) Case-2-d (MF).

A constraint approach is used for converting the multiobjective problem to a single objective problem. If a feasible solution with uniform member lengths exists, then the strain energy is minimized under constraint on the member lengths; otherwise, the variance of member length is minimize under constraint on strain energy.

It has been shown in the numerical examples that the triangular grid with uniform member lengths turns out to be a cylindrical surface with equilateral triangles. By contrast, the optimal shapes for quadrilateral grid are highly dependent on the initial solutions, and there exists a kind of bifurcation for the local optimal solutions in the objective function space. Finally, various shapes with uniform member lengths are found for the latticed shell with hexagonal grids.

References

[1] E. Ramm, and G. Mehlhorn, On shape finding methods and ultimate load analysis of reinforced concrete shells, Eng. Struct., Vol.13, pp.178.198, 1991.

[2] M. Ohsaki, T. Ogawa and R. Tateishi, Shape optimization of curves and surfaces considering fairness metrics and elastic stiffness, Struct Multidisc Optim, No.27, 250-258, 2004.
[3] S. Fujita and M. Ohsaki, Shape optimization of free-form shells using invariants of parametric surface, Int. J. Space Struct., Vol. 25, pp. 143-157, 2010.
[4] S. Fujita and M. Ohsaki, Shape optimization of shells considering strain energy and algebraic invariants of parametric surface, J. Struct. Constr. Eng., AIJ, Vol. 74, No. 639, pp. 841-847, 2009. (in Japanese)
[5] M. Ohsaki and M. Hayashi, Fairness metrics for shape optimization of ribbed shells, J. Int. Assoc. Shells and Spatial Struct., Vol. 41(1), pp. 31-39, 2000.
[6] H. Ohmori and H. Hamada, Computational morphogenesis of shells with free curved surface considering both designer's preference and structural rationality, Proc. Int. Assoc. Shell and Spatial Struct. (IASS-APCS 2006), Beijing, pp. 512-513, 2006.
[7] M. Ohsaki, T. Nakamura and M. Kohiyama, Shape optimization of a double-layer space truss described by a parametric surface, Int. J. Space Struct., Vol. 12(2), 1997.
[8] T. Ogawa, M. Ohsaki, R. Tateishi, Shape optimization of single-layer latticed shells for maximum linear buckling loads and uniform member lengths, J. Struct. Constr. Eng., AIJ, No. 570, pp. 129-136, 2003. (in Japanese)
[9] T. Wester, A geodesic dome-type based on pure plate action, Int. J. Space Struct., Vol. 5(2/3), pp. 155-167, 1990.
[10] J. P. Rizzuto, Rotated mutually supported elements in truncated icosahedric domes, J. Int. Assoc. Shell and Spatial Struct., Vol. 48(1), pp. 3-17, 2007.
[11] M. Turrin, P. von Buelow, A. Kilian and S. Sariyildiz, Performance-based design of SolSt: a roof system integrating structural morphology and solar energy transmittance, Proc. Int. Assoc. Shell and Spatial Struct. (IASS-2010), Shanghai, pp. 2991-3003, 2010.
[12] M. Eigensata, M. Deuss, A. Schiftner, M. Kilian, N. J. Mitra, H. Pottmann and M. Pauly, Case studies in cost-optimized paneling of architectural freeform surfaces, in: Advances in Architectural Geometry 2010, pp.49-72, Springer, 2010.
[13] P. E. Gill, W. Murray and M. A. Saunders, SNOPT: An SQP algorithm for large-scale constrained optimization, SIAM J. Optim., 12, 979-1006, 2002.